Nuclear Instruments and Methods in Physics Research A276 (1989) 456–467
North-Holland, Amsterdam

ON THE ENERGY RESOLUTION OF ELECTROMAGNETIC SAMPLING CALORIMETERS

J. DEL PESO
Universidad Autónoma de Madrid, Spain

E. ROS
DESY, Hamburg, FRG

Received 28 July 1988 and in revised form 31 October 1988

We investigate the energy resolution of electromagnetic sampling calorimeters using the Monte Carlo program EGS. We study how the energy resolution depends on the shower energy, on the thickness of the absorber and detector layers, and on the charge number and density of the materials used to construct the calorimeter. Finally we compare our Monte Carlo results with experimental data.

1. Introduction

Electromagnetic calorimeters [1] are nowadays standard devices in high energy physics. We can easily classify them into two categories: homogeneous calorimeters, made of a single material like lead glass, NaI, BGO, etc., and sampling calorimeters, with alternating layers of a passive material or absorber, and an active material or detector. The energy resolution of a calorimeter of the first type is limited by intrinsic fluctuations. For a calorimeter of the second type there is a second contribution to the energy resolution coming from the sampling fluctuations. Many different readout detectors have been employed in sampling calorimetry such as scintillator [2], liquid argon [3] and gas readout [4]. More recently also room temperature liquids [5] and silicon detectors [6] are under study. As absorber material, lead has been extensively used. Iron [7], uranium [8] and, to a minor extent, copper [9] have also been used, mainly in connection with hadronic calorimetry. More exotic materials like tungsten [10] have been introduced to obtain very compact calorimeters, especially if silicon is used as readout material. Low-Z absorbers have also been considered, but only for very special purposes [11].

Parallel to the development of the experimental techniques, Monte Carlo programs have been written to reproduce accurately electromagnetic showers in many different media. Starting with the shower program of Nagel [12] and the first versions of EGS [13], these programs have considerably grown in complexity and, at the same time, in predictive power. More recently and after the release of the latest version of EGS, called EGS4 [14], a comparison of Monte Carlo calculations with experimental data at the percent level has become possible.

In this article we first review present theoretical ideas about the energy resolution of electromagnetic sampling calorimeters. We confront them with Monte Carlo calculations using the EGS4 code, and finally with existing experimental data.

2. Parametrisation of the energy resolution

The experimental data suggest the following parametrisation of the energy resolution for electromagnetic sampling calorimeters:

$$\frac{\sigma_s}{E_s} = R\sqrt{\frac{\tau}{E}}\,, \tag{1}$$

where E is the energy (in GeV) of the showering particle (electron or photon), E_s and σ_s are respectively the visible (or sampled) energy in the calorimeter and its rms resolution, τ is the absorber thickness in radiation lengths, and R a constant that depends on the absorber material used. In ref. [15], for example, it is found that, in the case of scintillator calorimeters, $R \approx 14\%$ if lead is used as absorber, and $R \approx 17\%$ if iron is used (see also ref. [16] for the lead case).

A detailed analysis of the theoretical arguments leading to such a formula can be found in ref. [17] and will only be summarised here. It is assumed that most of the energy deposited in the active medium by the electromagnetic shower is carried by electrons behaving as minimum ionising particles. The number of "crossings" through the active medium layers by these electrons is:

$$N_c = \frac{E_s}{(\mathrm{d}E/\mathrm{d}x)_s s}\,,$$

0168-9002/89/$03.50

where s is the thickness of the active medium layers and $(dE/dx)_s$ the energy deposited by minimum ionising particles per unit length in this medium. The visible energy E_s can approximately be computed by the formula:

$$\frac{E_s}{E} \approx \frac{(dE/ds)_s s}{(dE/dx)_s s + (dE/dx)_t t},$$

where t is the thickness of the absorber layers. This formula assumes that the shower is only composed of minimum ionising particles. Since the energy deposited in the active medium is normally much smaller than the energy deposited in the absorber, it can be neglected. We obtain then:

$$N_c \approx \frac{E}{(dE/dx)_t t}.$$

The number of crossings N_c fluctuates from shower to shower and as a result the visible energy E_s also fluctuates. Assuming that these fluctuations are Gaussian and the crossings independent, we obtain:

$$\frac{\sigma_s}{E_s} = \frac{\sqrt{N_c}}{N_c} = \frac{1}{\sqrt{N_c}} = \sqrt{\frac{(dE/dx)_t t}{E}}$$

$$= 3.2\% \sqrt{\frac{\Delta E(\mathrm{MeV})}{E(\mathrm{GeV})}},$$

where ΔE is the energy lost per layer by a minimum ionising particle. In the following E will be given in units of GeV according to the standard prescription. Since $(dE/dx)_t = \epsilon_t / X_0$ where ϵ_t is the critical energy of the absorber and X_0 its radiation length, the previous formula can also be written in the following way:

$$\frac{\sigma_s}{E_s} = \sqrt{\frac{t}{X_0}\frac{\epsilon_t}{E}} = R\sqrt{\frac{\tau}{E}}$$

with

$$R = 3.2\% \sqrt{\epsilon_t(\mathrm{MeV})}.$$

Since the critical energy of lead is $\epsilon_t = 7.2$ MeV, we obtain $R = 8.5\%$ for lead absorbers. As noted in ref. [17], this formula has to be corrected for multiple scattering, which results in a spreading of the electron directions and other effects which imply a reduction of the visible energy. Taking them into account, the following corrected values of R are obtained: 23.0% for aluminium, 16.1% for iron, and 13.2% for lead.

The fluctuation in the number of crossings is normally the main component of the energy fluctuation but not the only one. Path length and Landau fluctuations should also be added but they are only important if a gas is used as active medium. These fluctuations can also be computed [17] and the resulting formulas agree well with experimental data, as shown for liquid argon calorimeters in ref. [3], for gaseous calorimeters in ref. [4], and for various types of calorimeters in ref. [1].

The most relevant implications of the formula $\epsilon_s/E_s = R\sqrt{\tau/E}$, with $R \sim \sqrt{\epsilon_t}$, are:

(1) σ_s/E_s varies like $1/\sqrt{E}$,

(2) σ_s/E_s, varies like $\sqrt{\tau}$ with no significant dependence on the active medium layer thickness,

(3) σ_s, E_s varies like $1/\sqrt{Z_t}$ where Z_t is the charge number of the absorber (the critical energy ϵ of a medium is proportional to $1/Z$).

In the following sections we will check whether these predictions are in agreement with detailed Monte Carlo calculations performed with EGS4.

3. Some remarks about the use of EGS

The EGS Monte Carlo code (see refs. [13] and [14]) is a system of computer codes for the simulation of electromagnetic showers produced by electron and photons in an arbitrary geometry. The different processes occurring in these showers are taken into account for particle energy ranges from a few keV to several TeV. In the EGS3 version of the program, the minimum energies (or cutoff energies) for secondary electrons and photons are 1 and 0.1 MeV respectively. Below these cutoff values, the energy of the particle is deposited in place without any further transport. In the EGS4 version of the program, the cutoff values can be as low as 0.010 MeV (kinetic energy) for electrons and 0.001 MeV for photons. The cross sections of the different processes used in the simulation have to be valid down to these energies. It should be noted that EGS4 offers the option to include Rayleigh scattering. Another important feature of the EGS4 version is the optimisation of the step size used for the particle transport. The importance of an adequate step size has been emphasized in ref. [18], in particular for the transport of low energy particles (below 20 MeV). The tuning of this step size can be achieved via the variable ESTEPE which defines a fixed fractional energy loss per step. The recommended values are 0.3% and 1% for high-Z and low-Z materials, respectively [14].

In order to evaluate the importance of these cutoff energies and step sizes, we have generated 250 electron showers of 1 GeV using the EGS4 code for each one of the following lead–scintillator sampling calorimeters:

(a) $t = 5.0$ mm and $s = 5.0$ mm,

(b) $t = 0.2$ mm and $s = 5.0$ mm,

(c) $t = 5.0$ mm and $s = 0.2$ mm,

where t is the thickness of the lead layers and s the thickness of the scintillator layers. The total depth of the calorimeter was kept constant at $30 X_0$ and the layers were considered laterally infinite (this is the so-called "semi-infinite" geometry). The statistical error expected for such a number of events is about 4%. The energy resolution σ_s/E_s is displayed as a function of the

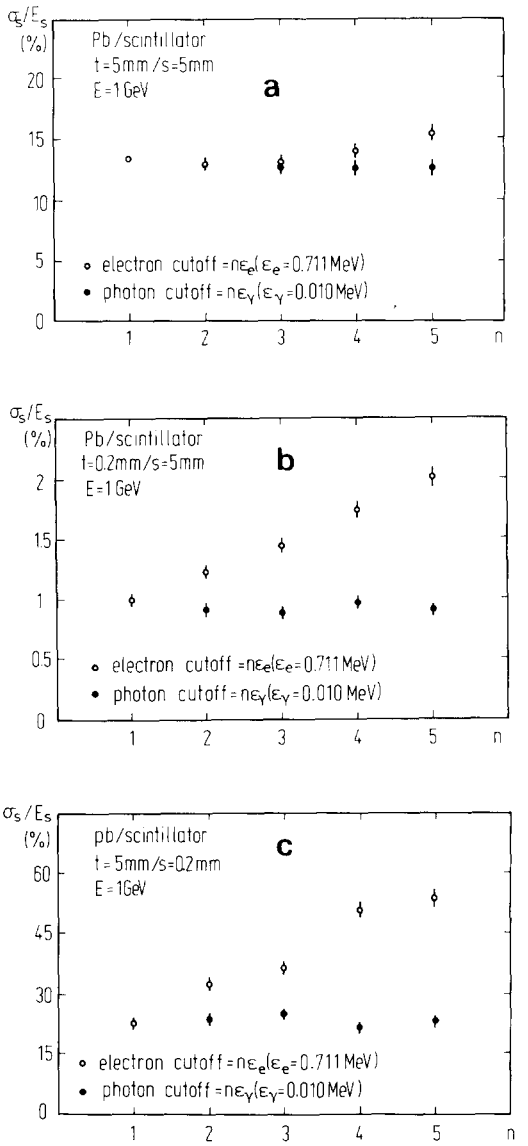

Fig. 1. (a) Electron and photon cutoff dependence of the energy resolution for a lead–scintillator calorimeter with $t = 5$ mm and $s = 5$ mm. (b) Electron and photon cutoff dependence of the energy resolution for a lead–scintillator calorimeter with $t = 0.2$ mm and $s = 5$ mm. (c) Electron and photon cutoff dependence of the energy resolution for a lead–scintillator calorimeter with $t = 5$ mm and $s = 0.2$ mm.

cutoff energies $n\epsilon_e$ and $n\epsilon_\gamma$, for electrons and photons, in figs. 1a–c. The minimum cutoff values used are $\epsilon_e = 0.711$ MeV and $\epsilon_\gamma = 0.010$ MeV (corresponding to $n = 1$). The cutoff energy for electrons includes of course the rest mass (0.511 MeV). We observe that for calorimeter a, the energy resolution is insensitive (within statistical errors) to the electron cutoff energy up to a value $n \approx 3$. For $n = 5$ the energy resolution has increased by 15%. In the case of calorimeters *b* and *c* where either the absorber or the detector are very thin, the energy resolution is very sensitive to the electron cutoff energy and increases by 50% or more from $n = 1$ to $n = 5$. On the other hand, no significant influence of the photon cutoff energies is observed for any of these three calorimeters. We note, however, that $n = 5$ corresponds to a cutoff energy of 0.05 MeV in the photon case, but to 3.6 MeV in the case of electrons. Since in the following we will consider calorimeters with thin layer thicknesses and since our aim is to obtain accurate values of the energy resolution, we conclude that a cutoff energy as low as possible has to be used. On the other hand, the computing time needed for the simulation increases for example by a factor 4 when going from $n = 2$ to $n = 1$ in the electron cutoff. For all these reasons, in the rest of the paper we will use 0.711 MeV as default cutoff for electrons. For photons the value 0.01 MeV will be used since no significant gain in computing time can be obtained by increasing it.

We have also investigated for the same three lead–scintillator calorimeters the dependence of the energy resolution on the variable ESTEPE previously defined. We do not observe any significant variation of the energy resolution when this variable is changed around the values of 0.3% and 1% for absorber and detector respectively. Since no spectacular gain in computing time can be achieved by slightly increasing these values, we will use them as default in the rest of the paper.

We finally remark that all the energy deposited in the active medium will be assumed to turn into visible energy. In this way we suppress any intrinsic fluctuation. As discussed elsewhere [17], these intrinsic fluctuations are normally much smaller than the sampling fluctuations. Our definition of sampling fluctuation is any fluctuation of the visible energy as calculated by the Monte Carlo program. We therefore include in it the so-called Landau and track length fluctuations.

4. Energy dependence

According to the theoretical considerations of section 2, the fluctuations σ_s of the visible energy E_s of a sampling calorimeter should scale with $\sqrt{E}$, E being the energy of the incident particle. In order to check this prediction we have generated showers in the energy range between 0.1 and 50 GeV for three different semi-infinite lead–scintillator sampling calorimeters:

(a) $t = 5.0$ mm $(0.9X_0)$ and $s = 5.0$ mm,

(b) $t = 20.0$ mm $(3.6X_0)$ and $s = 5.0$ mm,

(c) $t = 50.0$ mm $(8.9X_0)$ and $s = 5.0$ mm,

where t and s are the layer thicknesses of lead and scintillator, as before. All calorimeters had a depth of $30X_0$ ensuring full containment of the showers even at

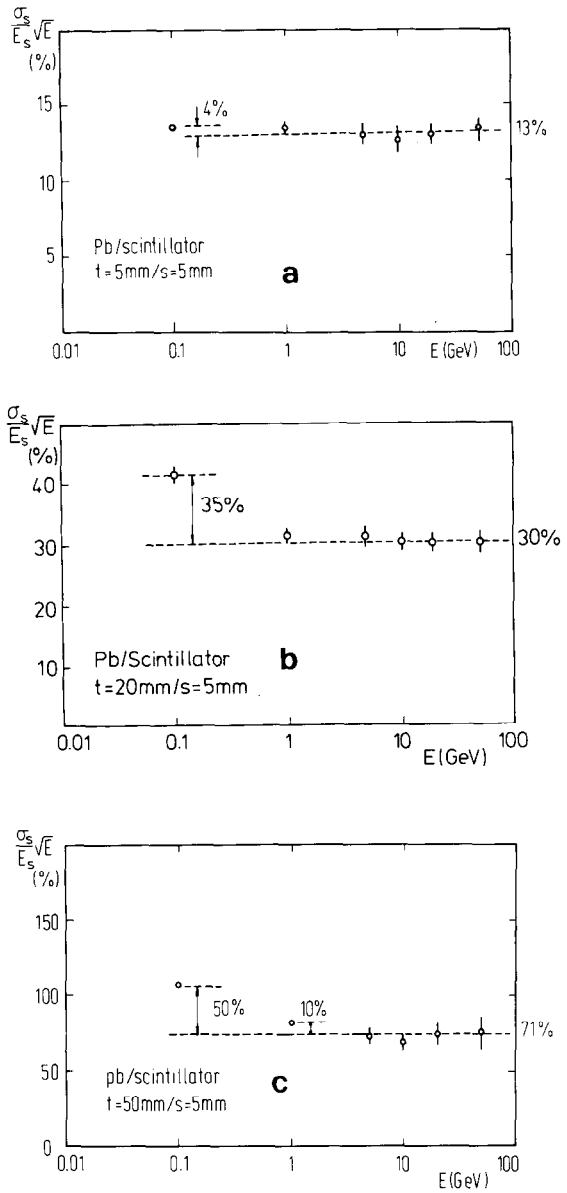

Fig. 2. (a) Energy dependence of the energy resolution for a lead–scintillator calorimeter with $t = 5$ mm and $s = 5$ mm. (b) Energy dependence of the energy resolution for a lead–scintillator calorimeter with $t = 20$ mm and $s = 5$ mm. (c) Energy dependence of the energy resolution for a lead–scintillator calorimeter with $t = 50$ mm and $s = 5$ mm.

the highest energies. The computing time needed in these calculations is proportional to the energy of the showers, in order to keep the statistical error, about 5%, approximately the same at all energies.

The results of these simulations are displayed in figs. 2a, 2b and 2c. We observe that for all calorimeters the quantity $(\sigma_s/E_s)\sqrt{E}$ reaches a constant value when the energy increases. These values are 13%, 30% and 70% respectively. At 1 GeV no significant deviation from this constant value is observed for calorimeters a and b, whereas a 12% increase of the resolution is observed for calorimeter c. At 0.1 GeV these deviations are 4%, 35% and 50% respectively. It is interesting to note that the deviations of the energy resolution from the $\sqrt{E}$ dependence at low energies go hand in hand with the deviations from linearity, as shown in figs. 3a, 3b and 3c. At 1 GeV calorimeter a shows a deviation from linearity of

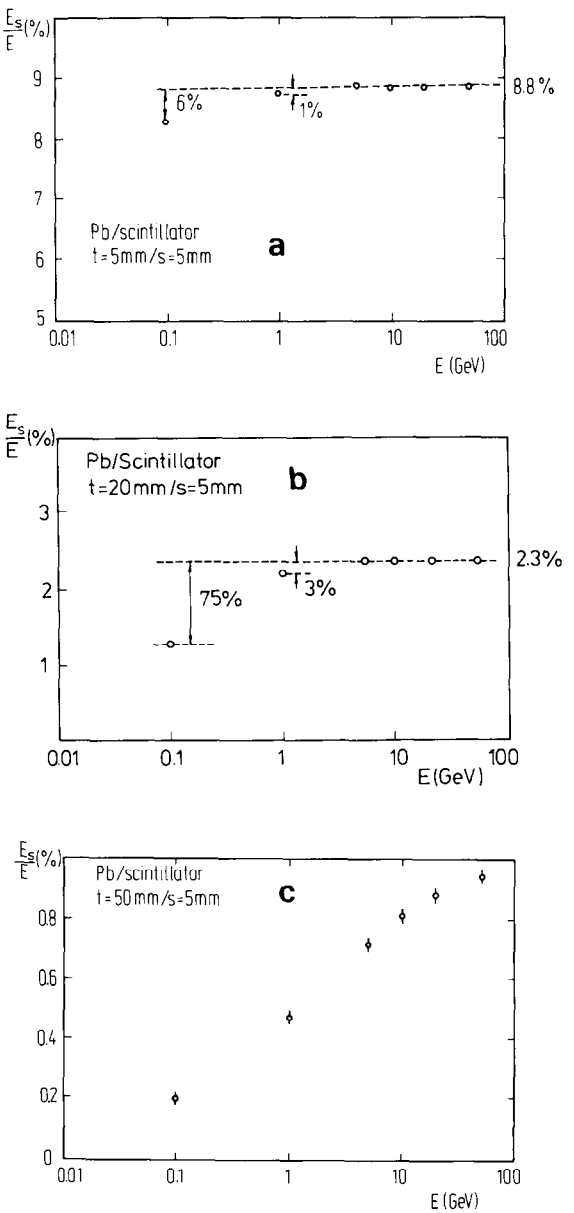

Fig. 3. (a) Linearity of response for a lead–scintillator calorimeter with $t = 5$ mm and $s = 5$ mm. (b) Linearity of response for a lead–scintillator calorimeter with $t = 20$ mm and $s = 5$ mm. (c) Linearity of response for a lead–scintillator calorimeter with $t = 50$ mm and $s = 5$ mm.

only 1%, but 6% at 0.1 GeV. Calorimeter c shows enormous deviations from linearity, even at high energies. This is not surprising since the absorber layer thickness is as large as $9X_0$. In order to limit the computing time needed, a compromise had to be found between the requirement of statistical precision in the calculations, which favours low energies, and the requirement that the response of the calorimeter should be linear with E and the energy resolution scale as $1/\sqrt{E}$. The latter requirements favour of course calculations at high energies. For these reasons all the computations have been performed for 1 GeV electron showers in the rest of the paper.

5. Thickness dependence

We have generated 1 GeV electron showers for lead–scintillator calorimeter with a constant scintillator layer thickness $s = 5$ mm, and lead layer thicknesses varying in the range between $t = 0.2$ mm ($0.04X_0$) and $t = 100$ mm ($18X_0$). All calorimeters had a fixed total depth of $30X_0$ but were laterally infinite. The statistical precision obtained in each computation of σ_s/E_s was about 5%.

The result of these simulations is shown in fig. 4a. The dependence of σ_s/E_s on t shows three different regions:

(1) For values of t between 1 and 10 mm, σ_s/E_s is well described by a straight line in the log/log plot. This means that σ_s/E_s is proportional to t^{α}. The value of α which gives the best fit is $\alpha = 0.66 \pm 0.02$.

(2) For values of t below 1 mm ($0.2X_0$), σ_s/E_s gets increasingly smaller than predicted by $t^{0.66}$.

(3) For values of t above 10 mm ($1.8X_0$), σ_s/E_s gets increasingly larger than predicted by $t^{0.66}$.

These calculations have been repeated for different values of the scintillator layer thickness s. We observe a dependence of the exponent α on s as indicated in fig. 4b.

Similarly, we have generated 1 GeV electron showers for lead–scintillator calorimeters with a constant lead layer thickness of $t = 5$ mm and scintillator layer thicknesses varying between $s = 0.2$ mm and $s = 100$ mm. The result is displayed in fig. 5a. The resolution σ_s/E_s is again well described by a curve of the type $s^{-\beta}$ with $\beta = 0.23 \pm 0.01$. The exponent β depends on t (lead layer thickness) as indicated in fig. 5b.

These results show that the formula $\sigma_s/E_s = R\sqrt{\tau/E}$ introduced in section 2, which assumes no dependence on the active material thickness, is in fact only a crude approximation. The dependence of σ_s/E_s on t and s over the large range of values considered before is complicated. However, for practical purposes, the typical values of t and s are limited in the range between 1 to 10 mm. In this region σ_s/E_s is well described by:

$$\frac{\sigma_s}{E_s} = \frac{\sigma_0}{\sqrt{E}} \frac{t^{\alpha}}{s^{\beta}},$$

σ_0, α and β being parameters only slightly dependent on s and t.

For practical purposes we will use in the following the formula:

$$\frac{\sigma_s}{E_s} = \frac{\sigma_0}{\sqrt{E}} \left(\frac{t}{X_t}\right)^{\alpha} \left(\frac{s}{X_s}\right)^{-\beta},$$

where X_t and X_s are the radiation lengths of the absorber and the detector respectively. In this way σ_0 has the same dimensions as the parameter R introduced in section 2. We emphasize that this formula is purely empirical and the parameters σ_0, α and β have to be determined by fitting Monte Carlo data, and not from first principles as in section 2.

In fig. 6 we plot the energy resolution of 12 different lead–scintillator calorimeters with lead layer thicknesses t equal to 1, 2, 5 and 10 mm and scintillator layer thicknesses of 1, 5 and 10 mm. The resolution of all these calorimeters has been determined by Monte Carlo simulations with a statistical precision of 10%. The best

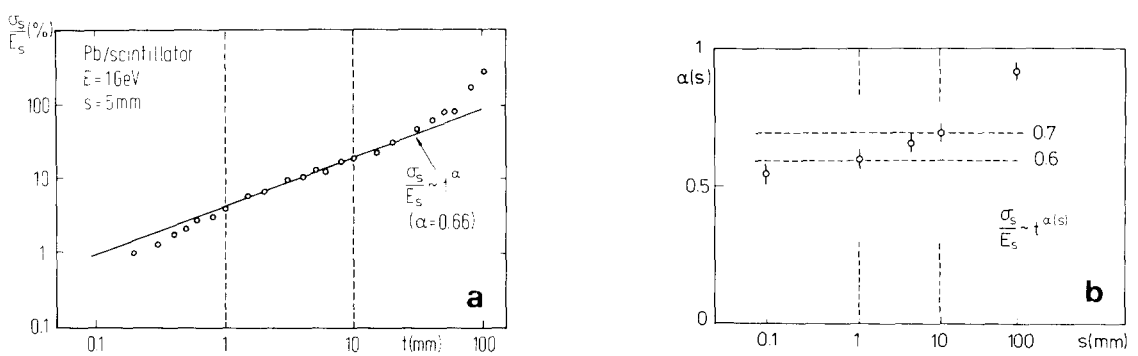

Fig. 4. (a) Dependence of the energy resolution of a lead–scintillator calorimeter with $s = 5$ mm on the absorber thickness. Both scales are logarithmic. (b) Dependence of the exponent α on the active material thickness.

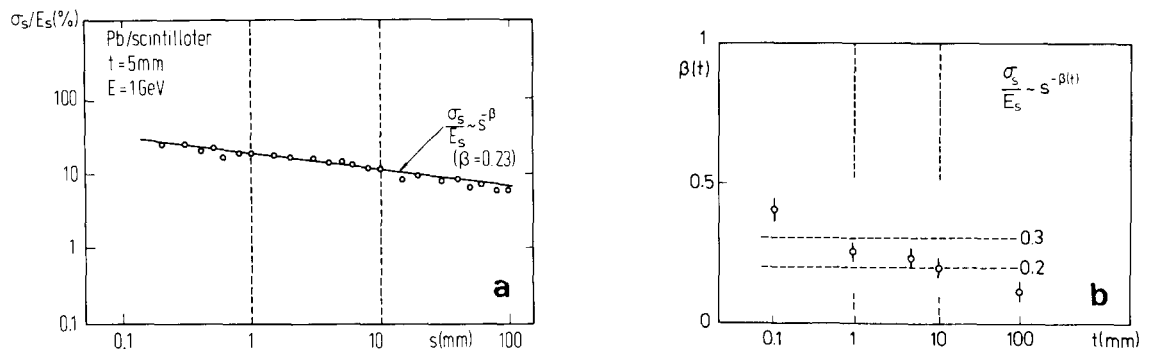

Fig. 5. (a) Dependence of the energy resolution of a lead–scintillator calorimeter with $t = 5$ mm on the detector thickness. Both scales are logarithmic. (b) Dependence of the exponent β on the absorber thickness.

fit of these resolutions by our empirical formula is obtained for the following values of σ_0, α and β:

$$\sigma_0 = 3.46 \pm 0.35\%, \quad \alpha = 0.67 \pm 0.03, \quad \beta = 0.29 \pm 0.03.$$

The formula of section 2, $\sigma_s/E_s = R(t/X_t)^{1/2}$, is also indicated in this plot. We observe that this formula gives a good description of the resolution for calorimeters with $s = 5$ mm, but fails to reproduce other values of s, since no dependence on s is assumed.

We can evaluate the systematic error made by considering that the parameters α and β are completely independent of s and t in the following way: let us assume that σ_0, α and β are perfectly known for a calorimeter with $t_0 = 3$ mm and $s_0 = 3$ mm, then for other values of t and s we have:

$$\frac{\sigma_s}{E_s} = \frac{\sigma_0}{\sqrt{E}} \left(\frac{t}{t_0}\right)^{\alpha} \left(\frac{s}{s_0}\right)^{-\beta},$$

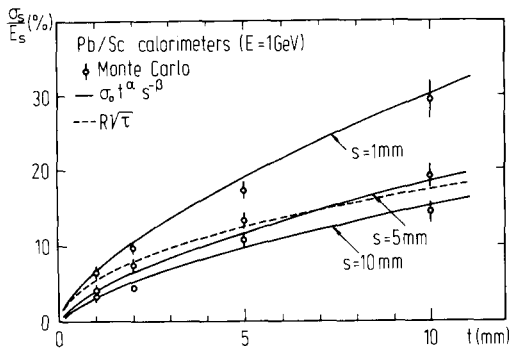

Fig. 6. Energy resolution for 1 GeV electron showers of a lead–scintillator calorimeter for various absorber and detector thicknesses. The points are Monte Carlo data, the full line is a fit to the formula given in section 5, and the dashed line is the formula given in section 2.

and therefore:

$$\frac{\Delta\sigma_s}{\sigma_s} = \Delta\alpha\left(\log\frac{t}{t_0}\right) - \Delta\beta\left(\log\frac{s}{s_0}\right),$$

where $\Delta\alpha$ and $\Delta\beta$ are the differences between the exact values of these parameters for a calorimeter with layer thicknesses t and s, and the values for t_0 and s_0. In fig. 4b and 5b we observe that for t and s in the range between 1 and 10 mm we have: $\alpha \approx 0.65 \pm 0.05$ and $\beta \approx 0.25 \pm 0.05$. This implies a maximum systematic error in σ_s of 11% and an average systematic error of 4%.

We also remark that the statistical error expected in the calculation of the energy resolution is:

$$\left(\frac{\Delta\sigma_s}{\sigma_s}\right)^2 = \left(\frac{\Delta\sigma_0}{\sigma_0}\right)^2 + (\Delta\alpha)^2(\log t)^2 + (\Delta\beta)^2(\log s)^2 + 2\left(\frac{\Delta\sigma_0}{\sigma_0}\Delta\alpha\right)\log t - 2\left(\frac{\Delta\sigma_0}{\sigma_0}\Delta\beta\right)\log s - 2(\Delta\alpha\Delta\beta)\log s \log t.$$

Taking into account the statistical errors of σ_0, α and β and the correlation errors given by the fit, we obtain for the previous computations a statistical error of about 5% for values of t and s in the range between 1 and 10 mm.

We have repeated the calculation of the parameters σ_0, α and β for 10 GeV incident electrons. The result is compatible within errors with the previous one obtained at 1 GeV.

6. Z dependence

We have calculated the parameters σ_0, α and β introduced in the previous section for different calorimeters using scintillator as active material and absorbers

Table 1a
Charge number, density and radiation length of various materials used as absorbers

Material	Z	ρ [g/cm^3]	X_0 [mm]
C	6	2.27	188.5
Al	13	2.70	88.9
Fe	26	7.87	17.6
Sn	50	7.31	12.1
W	74	19.30	3.5
Pb	82	11.35	5.6
U	92	18.95	3.2

Table 1b
Charge number, density and radiation length of various materials used as active materials

Material	Z	ρ [g/cm^3]	X_0 [mm]
Liquid He	2	0.13	7546
TMS	(2.9)	0.65	525
Scintillator	(3.4)	1.03	424
Silicon	14	2.33	93
Liquid Ar	18	1.40	140

with charge number going from $Z = 6$ (carbon) to $Z = 92$ (uranium). The charge number Z, density ρ and radiation length X_0 of these materials is listed in table 1a. The procedure to obtain σ_0, α and β is similar to the one used for lead in the previous section: the resolution for 1 GeV electron showers of 12 calorimeters with $s = 1$, 5 and 10 mm scintillator layer thickness, and absorber layer thicknesses of 0.2, 0.4, 1 and $2\,X_0$, is calculated with 10% statistical precision. Then the formula

$$\frac{\sigma_s}{E_s} = \frac{\sigma_0}{\sqrt{E}} \left(\frac{t}{X_t}\right)^{\alpha} \left(\frac{s}{X_s}\right)^{-\beta}$$

is fitted to the 12 values. The resulting parameters are listed in table 2a and in fig. 7a and 7b. We note that for $Z > 25$ the exponents α and β are constant within errors, and that σ_0 scales like $1/\sqrt{Z}$ in agreement with

Table 2a
Values of the parameters σ_0, α and β obtained from fits to Monte-Carlo data for various calorimeters using scintillator as active material

Absorber	Detector	σ_0 [%]	α	β
C	Scintillator	16.48 ± 2.50	0.72 ± 0.03	0.16 ± 0.02
Al	Scintillator	11.02 ± 1.21	0.70 ± 0.03	0.15 ± 0.02
Fe	Scintillator	6.33 ± 0.52	0.62 ± 0.03	0.21 ± 0.02
Sn	Scintillator	4.53 ± 0.32	0.65 ± 0.03	0.25 ± 0.03
W	Scintillator	3.61 ± 0.17	0.70 ± 0.03	0.29 ± 0.03
Pb	Scintillator	3.46 ± 0.19	0.67 ± 0.03	0.29 ± 0.03
U	Scintillator	3.28 ± 0.15	0.67 ± 0.03	0.30 ± 0.03

Table 2b
Values of the parameters σ_0, α and β obtained from fits to Monte Carlo data for various calorimeters using lead as absorber

Absorber	Detector	σ_0 [%]	α	β
Pb	Liquid He	5.68 ± 0.59	0.62 ± 0.03	0.17 ± 0.03
Pb	TMS	4.43 ± 0.26	0.71 ± 0.03	0.26 ± 0.03
Pb	Scintillator	3.46 ± 0.19	0.67 ± 0.03	0.29 ± 0.03
Pb	C	3.55 ± 0.16	0.65 ± 0.03	0.30 ± 0.03
Pb	Si	5.04 ± 0.20	0.66 ± 0.03	0.24 ± 0.03
Pb	Liquid Ar	6.49 ± 0.31	0.62 ± 0.03	0.19 ± 0.03
Pb	Fe	7.76 ± 0.47	0.62 ± 0.03	0.18 ± 0.03
Pb	Sn	9.49 ± 0.70	0.62 ± 0.03	0.16 ± 0.03
Pb	Pb	7.53 ± 0.76	0.57 ± 0.03	0.20 ± 0.03

the theoretical prediction made in section 2 for the parameter R.

Similarly we have calculated σ_0, α and β for lead calorimeters containing active media with a charge number going from $Z = 2$ (liquid helium) to $Z = 82$ (lead). The material constants used in these calculations are listed in tables 1a and 1b, and the results listed in

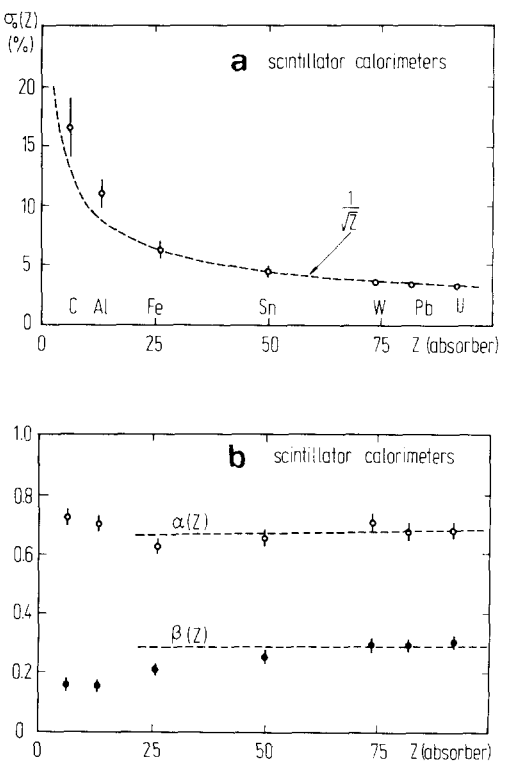

Fig. 7. (a) The parameter σ_0 as a function of the absorber charge number Z, for various calorimeters using scintillator as active material. (b) The exponents α and β as a function of the absorber charge number Z, for various calorimeters using scintillator as active material.

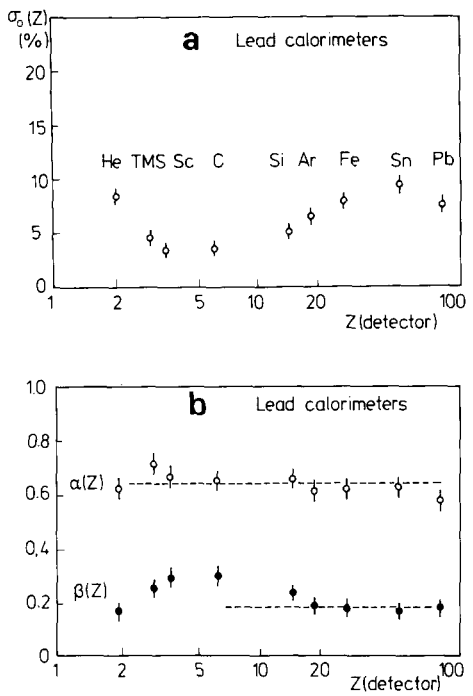

Fig. 8. (a) The parameter σ_0 as a function of the detector charge number Z, for various calorimeters using lead as absorber. (b) The exponents α and β as a function of the detector charge number Z, for various calorimeter using lead as absorber.

table 2b and plotted in figs. 8a and 8b. In practice only low-Z materials have been experimentally used so far as active media. We observe in this case a strong dependence of σ_0, α and β on the charge number Z of the active material, in particular for low Z values.

7. Density dependence

The formula $\sigma_s/E_s = R(t/X_t)^{1/2}$ of section 2, with $R \sim 1/\sqrt{Z}$, implies no dependence of σ_s on the density of the absorber, apart, of course, from the one contained in X_t. We have also investigated if in our formula of section 5 the whole density dependence is contained in X_t and X_s. In other words, we have investigated how σ_0, α and β depend on the density of the calorimeter materials.

For these purpose we have calculated these three parameters for several lead–scintillator calorimeters, following the method described in previous sections and for the following material parameters:

(a) the scintillator density is kept constant at its nominal value (1.032 g/cm^3) and the lead density is varied between 1 and 20 g/cm^3,

(b) the lead density is kept constant at its nominal value (11.3 g/cm^3) and the scintillator density is varied between 0.1 and 10 g/cm^3.

The result of these simulations is plotted in figs. 9a and 9b for the case of lead of varying density, and in figs. 10a and 10b for the case of scintillator of varying density. We observe, within our statistical errors, no significant dependence of σ_0, α and β on the density of the materials used in the simulation. Lead and scintillator of varying density cannot, of course, exist in nature. However, the Monte Carlo program also allows to simulate them.

8. Comparison with experiment

In order to compare our EGS based formula with experimental results, we have selected a large number of energy resolution measurements performed over the last 15 years with electromagnetic calorimeters made of lead, iron or uranium as absober, and scintillator or liquid argon as active material. The measurements are listed in tables 3a and 3b.

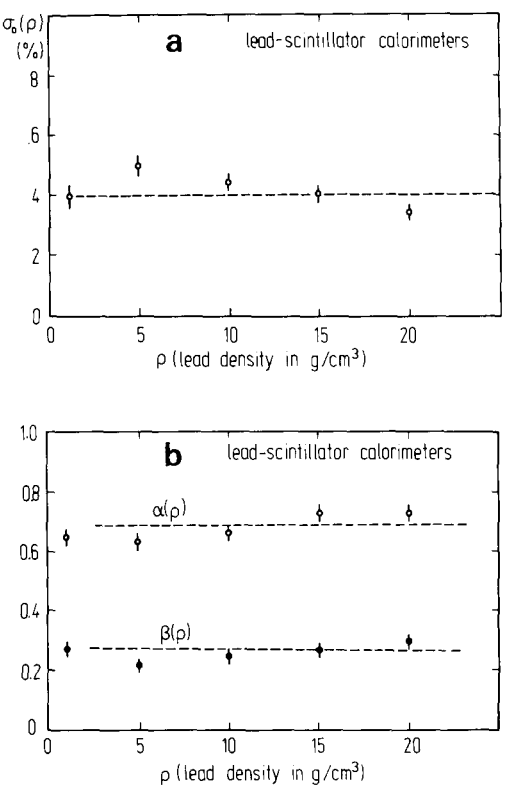

Fig. 9. (a) The parameter σ_0 as a function of the lead density ρ, for various calorimeters using scintillator as active material. (b) The exponents α and β as a function of the lead density ρ, for various calorimeters using scintillator as active material.

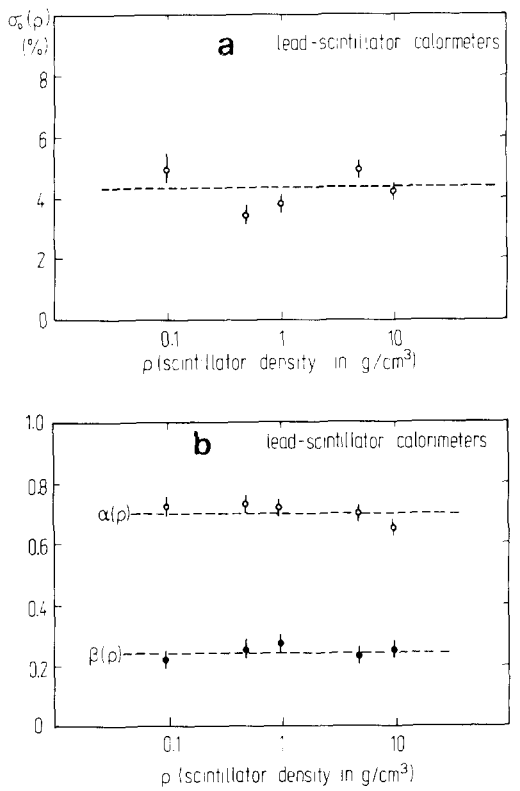

Fig. 10. (a) The parameter σ_0 as a function of the scintillator density ρ, for various calorimeters using lead as active material. (b) The exponents α and β as a function of the scintillator density ρ, for various calorimeters using lead as active material.

Ideally a good measurement of the energy resolution should satisfy the following requirements:

- The calorimeter should have a regular sampling structure with no mixture of absorbers or active materials. The layers should have a fixed thickness.
- No additional dead materials should be present in front or inside the calorimeter.
- The calorimeter should provide full containment of the showers. In particular the depth should be at least $20 X_0$.
- The measurements should be performed over a wide range of energies, and energies below 1 GeV should be ignored in the analysis.
- The experimental result should be carefully corrected for instrumental effects (electronic noise, calibration errors, photostatistics, etc.).

In practice almost none of the measurements listed in tables 3a and 3b fulfil all these requirements. This has to be taken into account when comparing with the Monte Carlo predictions. In the case of scintillator readout, the fluctuation in the number of photoelectrons is the main effect which adds to the sampling fluctuations. This contribution has been subtracted from

Table 3a
Measured and calculated energy resolutions for various calorimeters employing scintillator as active material. The values given for σ are fractional energy resolutions scaled to 1 GeV showers. The contribution of photoelectron statistics has been subtracted to the measured values. Otherwise they appear in parentheses.

Absorber	t [mm]	s [mm]	σ_{exp} [%]	σ_{EGS} [%]	$\sigma_{exp}/\sigma_{EGS}$	Ref.
Pb	1.0	5.0	5.0	4.0	1.2	[20]
Pb	1.0	5.0	6.0	4.0	1.5	[24]
Pb	2.0	5.0	7.5	6.3	1.2	[25]
Pb	2.1	6.3	9.0	6.1	1.5	[15]
Pb	2.5	4.0	(10.5)	7.8	1.3	[26]
Pb	3.2	5.0	12.0	8.6	1.4	[27]
Pb	3.5	4.0	(14.0)	9.8	1.4	[28]
Pb	4.0	5.0	11.6	10.0	1.2	[29]
Pb	4.2	12.6	10.8	7.9	1.4	[15]
Pb	6.0	5.0	13.6	13.1	1.1	[30]
Pb	6.0	2.5	17.5	16.0	1.1	[31]
Pb	8.4	25.2	14.7	10.3	1.4	[15]
Pb	9.4	6.4	(18.2)	16.5	1.1	[32]
Pb	10.0	2.5	22.6	22.6	1.0	[33]
U	1.6	2.5	(11.0)	9.7	1.1	[34]
U	2.0	2.5	(13.9)	11.3	1.2	[35]
U	3.0	2.5	(16.3)	15.0	1.1	[36]
U	3.2	5.0	(14.8)	12.7	1.2	[37]
U	3.2	3.0	(15.0)	14.8	1.0	[37]
U	10.0	5.0	(28.0)	27.9	1.0	[38]
Fe	4.8	6.3	10.1	6.8	1.5	[15]
Fe	25.0	5.0	(23.0)	20.0	1.1	[7]

Table 3b
Measured and calculated energy resolutions for various calorimeters employing liquid argon as active material. The contributions of electronic noise and calibration errors have been subtracted to the measured values. Otherwise they appear in parentheses.

Absorber	t [mm]	s [mm]	σ_{exp} [%]	σ_{EGS} [%]	$\sigma_{exp}/\sigma_{EGS}$	Ref.
Pb	1.0	2.0	8.0	5.0	1.6	[39]
Pb	1.2	3.6	(8.5)	5.0	1.7	[40]
Pb	1.5	5.0	7.5	5.4	1.4	[41]
Pb	1.5	2.0	8.0	6.4	1.3	[42]
Pb	1.9	3.0	9.0	6.9	1.3	[43]
Pb	2.0	5.0	(10.0)	6.5	1.5	[44]
Pb	2.0	3.0	(10.8)	7.1	1.5	[45]
Pb	2.0	2.0	9.6	7.7	1.2	[46]
Pb	2.0	2.0	(10.3)	7.7	1.3	[47]
Pb	2.2	2.0	9.5	7.7	1.2	[48]
Pb	2.4	2.8	11.2	8.1	1.4	[43]
U	2.0	1.6	14.0	11.5	1.2	[49]
Fe	1.0	1.0	2.8	3.7	0.8	[50]
Fe	1.5	1.5	9.5	4.4	2.2	[51]
Fe	1.5	2.0	6.9	4.1	1.7	[52]
Fe	1.5	2.0	(7.4)	4.1	1.8	[53]
Fe	2.0	2.0	6.1	4.9	1.2	[46]

Table 3c
Measured and calculated energy resolutions for various calorimeters employing a gas as active material

Absorber	t [mm]	s [mm]	σ_{exp} [%]	σ_{EGS} [%]	$\sigma_{exp}/\sigma_{EGS}$	Ref.
Pb	1.1	5.0	11.2	14.0	0.8	[54]
Pb	1.3	12.7	17.0	13.0	1.3	[55]
Pb	1.4	10.0	14.0	14.0	1.0	[56]
Pb	2.0	6.0	15.0	18.4	0.8	[57]
Pb	2.0	3.2	16.0	20.5	0.8	[58]
Pb	2.8	11.6	17.0	19.5	0.9	[59]
Pb	2.8	12.4	17.5	19.3	0.9	[60]
Pb	2.8	9.5	17.0	20.2	0.8	[61]
Pb	3.0	7.0	24.0	22.0	1.1	[62]
Pb	5.0	9.0	28.0	27.4	1.0	[63]
Pb	6.0	2.0	27.0	38.8	0.7	[64]

the measured energy resolution whenever the information was available (otherwise the measured value appears in brackets). In the case of liquid argon readout, the main instrumental effects are electronic noise and calibration errors. Again these contributions have been subtracted whenever possible.

We estimate the errors in the values calculated from our EGS based formula to be about 5% systematic and 5% statistical (see the discussion in section 5). The errors in the measured values have not been quoted since the systematic errors, which are dominant, are difficult to estimate and are normally not given.

The ratios between the measured resolutions and the calculated ones are also listed in the tables. In general the measured resolutions are worse than the calculated ones. We attribute this fact to the instrumental effects mentioned before. It is significant that the measured energy resolution of calorimeters with a calculated value below $10\%/\sqrt{E}$ are worse by 50% on the average than the calculated value. Of course, these calorimeters are more sensitive to instrumental effects. The case of the ARGUS calorimeter is particularly interesting. With 1 mm lead and 5 mm scintillator layer thicknesses, it can theoretically achieve an energy resolution of $4\%/\sqrt{E}$, to be compared with a measured value of $7\%/\sqrt{E}$ [19]. However, after careful corrections for photostatistics and for energy leakage, a value of $5\%\sqrt{E}$ is obtained [20]. Calorimeters with an energy resolution above $10\%/\sqrt{E}$ are in general well reproduced by the EGS calculation. The agreement is typically better than 10%.

9. The case of gaseous calorimeters

Calorimeters with gaseous detectors [4] require a special treatment for the following reason: the density of gases is smaller by 3 orders of magnitude than the density of the solid or liquid materials considered up to now as active media. These small densities lead to a qualitatively different behaviour of the energy resolution. The dominant fluctuations are no longer the fluctuations in the number of crossings, as discussed in section 2, but rather the Landau fluctuations of the energy deposited by low energy electrons in each crossing and the path length fluctuations produced by electrons trapped in the gas layers. All these fluctuations produce a considerable degradation of the energy resolution in case a purely proportional mode is used for the readout. Attempts have been made to reduce these fluctuations, e.g. by operating in the limited streamer mode [21] with the aim to suppress Landau fluctuations by a saturation in the response of each calorimeter cell. This is practically achieved but at the price of losing linearity in the response. This type of readout is sometimes called "digital" readout [4]. The track length fluctuations can also be limited by adding walls able to stop low energy electrons. It is obvious that the particular readout technique will have a strong influence on the energy resolution of gaseous calorimeters.

From the simulation point of view, the fact that the range of delta rays is much longer in gases than in solids or liquids adds a new complication. According to ref. [22], the range r of low energetic electrons in a medium of density ρ can be approximated by the formula:

$$r = 0.75E^{1.72}/\rho$$

(r in cm, E in MeV, ρ in g/cm^3), E being the kinetic energy of electrons. The kinetic energy used as cutoff in the calculations reported above was 0.2 MeV, which implies a minimum range for electrons in scintillator of 0.4 mm. This value is in general much smaller than the layer thickness considered. In argon gas, a 0.2 MeV electron has a range of 25 cm. To obtain a similar minimum range of 0.4 mm a cutoff of 20 keV has to be used. This is certainly possible at the cost of a considerable increase in the computing time needed for the calculations. The necessity of using such low cutoff values to simulate gaseous detectors was pointed out a long time ago [23]. Fig. 11 shows how the energy resolution depends on the cutoff values for a calorimeter with lead as absorber ($t = 5$ mm) and argon gas ($s = 5$ mm) as active material. For an electron cutoff of 20 keV (kinetic energy) we obtain a resolution of about $30\%/\sqrt{E}$, whereas for the cutoff of 200 keV used in previous calculations we obtain $42\%/\sqrt{E}$.

A fit to the energy resolution of lead-argon gas calorimeters using the procedures described in section 5 and the cutoff value of 20 keV yields the following parameters:

$$\sigma_0 = 5.86 \pm 0.33\%, \quad \alpha = 0.51 \pm 0.02, \quad \beta = 0.17 \pm 0.03,$$

the radiation length of gaseous argon being 1.1×10^5 mm. In table 3b we compare the measured energy

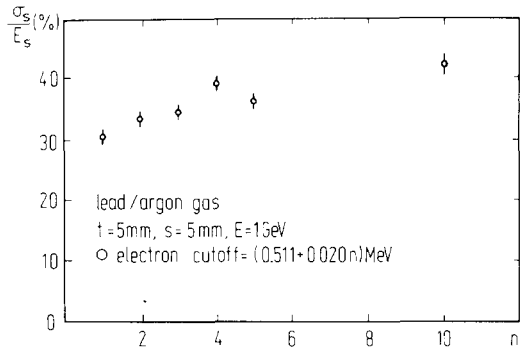

Fig. 11. Electron cutoff dependence of the energy resolution for a lead-argon gas calorimeter with $t = 5$ mm and $s = 5$ mm.

resolution of various gaseous electromagnetic calorimeters using lead as absorber, with the prediction of our EGS based formula. We observe in this case that in general the measured value is smaller than the predicted one. This is not surprising since, as discussed previously, part of the energy fluctuations can be reduced by an adequate choice of the readout technique.

10. Conclusions

We have studied the energy resolution of electromagnetic sampling calorimeters using the Monte Carlo program EGS4. We have found that for absorber and detector layer thicknesses t and s, the fractional energy resolution σ_s/E_s, can be approximately described by:

$$\frac{\sigma_s}{E_s} = \frac{\sigma_0}{\sqrt{E}} \left(\frac{t}{X_t}\right)^{\alpha} \left(\frac{s}{X_s}\right)^{-\beta},$$

E being the shower energy and X_t and X_s the radiation lengths of absorber and detector respectively. The other parameters appearing in this formula, σ_0, α and β, have to be adjusted to Monte Carlo data. We have found that α and β are rather independent of the density and charge number of the absorber. The parameter σ_0 scales with $1/\sqrt{Z_t}$, Z_t being the absorber charge number. Finally we have compared the predictions of this Monte Carlo based formula with existing experimental data. Good agreement is found in general within the limits imposed by expected instrumental effects in the energy resolution measurements.

Acknowledgement

We would like to thank G. Wolf for useful comments.

References

[1] C.W. Fabjan, CERN-EP/85-54 (1985).
[2] W. Schmidt-Parzefall, Phys. Scripta 23 (1981) 425.
[3] J. Engler, Nucl. Instr. and Meth. 225 (1984) 525.
[4] J. Engler, Nucl. Instr. and Meth. 217 (1983) 9; C.W. Fabjan, Nucl. Instr. and Meth. A252 (1986) 145.
[5] J. Engler and H. Keim, Nucl. Instr. and Meth. 223 (1984) 47.
[6] R. Klanner, Nucl. Instr. and Meth. A235 (1985) 209.
[7] H. Abramowicz et al., Nucl. Instr. and Meth. 180 (1981) 429.
[8] C.W. Fabjan et al., Phys. Lett. B60 (1975) 105.
[9] O. Botner et al., Nucl. Instr. and Meth. 179 (1981) 45.
[10] G. Barbiellini et al., Nucl. Instr. and Meth. 235 (1985) 55.
[11] A.N. Diddens et al., Nucl. Instr. and Meth. 178 (1980) 27.
[12] H. Nagel, Z. Phys. 186 (1965) 319.
[13] R.L. Ford and W.R. Nelson, SLAC-210 (1978).
[14] W.R. Nelson, H. Hirayama and D.O. Rogers, SLAC-265 (1985).
[15] S. Stone et al., Nucl. Instr. and Meth. 151 (1978) 387.
[16] G. Abshire et al., Nucl. Instr. and Meth. 164 (1979) 67.
[17] U. Amaldi, Phys. Scripta 23 (1981) 409.
[18] D.W.O. Rogers, Nucl. Instr. and Meth. A227 (1984) 535.
[19] W. Hofmann et al., Nucl. Instr. and Meth. 163 (1979) 77.
[20] W. Hofmann et al., Nucl. Instr. and Meth. 195 (1982) 475.
[21] E. Iarocci, Nucl. Instr. and Meth. 217 (1983) 30.
[22] H. Fesefeldt, PITHA 85/02 (1985).
[23] H.G. Fisher, Nucl. Instr. and Meth. 156 (1978) 81; A. Cattai et al., Nucl. Instr. and Meth. A235 (1985) 310.
[24] M.A. Schneegans et al., Nucl. Instr. and Meth. 193 (1982) 445.
[25] R. Klanner et al., ZEUS note 86-3, unpublished.
[26] G. Winter et al., Nucl. Instr. and Meth. A238 (1985) 307.
[27] F. Schoessow et al., DPF meeting, Santa Fe (1984).
[28] A. Beer et al., Nucl. Instr. and Meth. 360 (1984) 360.
[29] C. Daum et al., ZEUS note 86-13, unpublished.
[30] R. Klanner et al., ZEUS note 86-8, unpublished.
[31] F. Barreiro et al., Nucl. Instr. and Meth. A257 (1987) 145.
[32] J.P. Knauer and D.E. Yout, Nucl. and Instr. Meth. 129 (1975) 91.
[33] E. Bernardi et al., Nucl. Instr. and Meth. A262 (1987) 229.
[34] R. Carosi et al., Nucl. Instr. and Meth. 219 (1984) 311.
[35] T. Akesson et al., Nucl. Instr. and Meth. A241 (1985) 17.
[36] B. Anders et al., DESY 86-105 (1986).
[37] H. Tiecke et al., ZEUS note 87-39, unpublished.
[38] M.G. Catanesi et al., Nucl. Instr. and Meth. 260 (1987) 43.
[39] A. Delfosse et al., Nucl. Instr. and Meth. 156 (1978) 425.
[40] H.J. Behrend et al., Phys. Scripta 23 (1981) 610.
[41] H. Burkhardt et al., CERN-EP/87-166.
[42] J.H. Cobb et al., Nucl. Instr. and Meth. 158 (1979) 93.
[43] W. Braunschweig et al., DESY 87-98 (1987).
[44] A. Ladage, SLAC-250 (1982) 180.
[45] G.S. Abrams et al., IEEE Trans. Nucl. Sci. NS-25 (1978) 309.
[46] Y. Asano et al., Nucl. Instr. and Meth. 174 (1980) 357.
[47] C. Nelson et al., Nucl. Instr. and Meth. 216 (1983) 381.
[48] D. Hitlin et al., Nucl. Instr. and Meth. 137 (1976) 225.
[49] B. Cox, Fermilab-Conf. 86/14-E (1986).
[50] C. Cerri and F. Sergianpietri, Nucl. Instr. and Meth. 141 (1977) 207.

[51] B. Babaev et al., Nucl. Instr. and Meth. 160 (1979) 427.
[52] W.J. Willis and V. Radeka, Nucl. Instr. and Meth. 120 (1974) 221.
[53] C. Fabjan et al., Nucl. Instr. and Meth. 141 (1977) 61.
[54] A. Barbaro Galtieri et al., Nucl. Instr. and Meth. 213 (1983) 223.
[55] D. Andrews et al., Nucl. Instr. and Meth. 211 (1983) 47.
[56] M. Bergreen et al., Nucl. Instr. and Meth. 225 (1984) 477.
[57] G. Battistoni, Gas Calorimetry Conf., Batavia (1982).
[58] H. Videau, Nucl. Instr. and Meth. 225 (1984) 481.
[59] R. Fabrizio et al., Nucl. Instr. and Meth. 227 (1984) 220.
[60] W. Toki et al., Nucl. Instr. and Meth. 219 (1984) 479.
[61] R.L. Anderson et al., IEEE Trans. Nucl. Sci. NS-25 (1978) 340.
[62] Y. Hayashide et al., Nucl. Instr. and Meth. 227 (1984) 452.
[63] G. Battistoni et al., SLAC-250 (1982).
[64] G. Bella et al., Nucl. Instr. and Meth. A252 (1986) 503.